Raman scattering study of the anharmonic effects in CeO_{2-y} nanocrystals

2007 J. Phys.: Condens. Matter 19 496209

(http://iopscience.iop.org/0953-8984/19/49/496209)

IOP PUBLISHING JOURNAL OF PHYSICS: CONDENSED MATTER

J. Phys.: Condens. Matter **19** (2007) 496209 (9pp) doi:10.1088/0953-8984/19/49/496209

Raman scattering study of the anharmonic effects in CeO_{2-y} nanocrystals

Z V Popović[1], Z Dohčević-Mitrović[1], A Cros[2] and A Cantarero[2]

[1] Center for Solid State Physics and New Materials, Institute of Physics, Pregrevica 118, 11080 Belgrade, Serbia
[2] Materials Science Institute, University of Valencia, P O Box 22085, E-46071, Valencia, Spain

Received 3 May 2007, in final form 17 October 2007
Published 12 November 2007
Online at stacks.iop.org/JPhysCM/19/496209

Abstract

We have studied the temperature dependence of the F_{2g} Raman mode phonon frequency and broadening in CeO_{2-y} nanocrystals. The phonon softening and phonon linewidth are calculated using a model which takes into account the three-and four-phonon anharmonic processes. A detailed comparison of the experimental data with theoretical calculations revealed the predominance of four-phonon anharmonic processes in the temperature dependence of the phonon energy and broadening of the nanocrystals. On the other hand, three-phonon processes dominate the temperature behavior of phonons in polycrystalline samples. The anti-Stokes/Stokes peak intensity ratio was also investigated and found to be smaller for nanosized CeO_2 powders than in the bulk counterpart.

(Some figures in this article are in colour only in the electronic version)

1. Introduction

Raman spectroscopy is a powerful tool for characterization of nanosized materials and structures. This technique is widely used for the study of phonon confinement, strain and substitutional effects, porosity, and nonstoichiometry in different kinds of nanomaterials. Recent progress in the use of Raman spectroscopy for nanomaterial characterization is given in [1]. Very few experiments have been carried out to investigate the temperature dependence of Raman mode frequencies and linewidths in nanocrystals [2, 3]. Finite-size effects in nanocrystals are expected to modify the anharmonicity and the phonon decay times. From the temperature-dependent Raman scattering study of nanocrystalline and bulk silicon Mishra and Jain [2] found a higher degree of anharmonicity in Si nanocrystals in comparison with bulk, while Spanier *et al* [4] reported that phonon coupling is not stronger in the CeO_{2-y} nanoparticle system than that in the bulk counterpart. In addition, to the best of our knowledge, the anharmonicity in very small nanocrystals has not been investigated theoretically yet.

Cerium dioxide (CeO_2) has recently attracted a lot of interest as a potential electrolyte in intermediate-temperature solid oxide fuel cells (SOFCs) due to its ability to absorb and release oxygen easily and to exhibit higher ionic conductivity at lower temperatures (500–700 °C) than conventional yttria-stabilized zirconia (YSZ). Therefore it is important to investigate its characteristics at elevated temperatures.

The purpose of this paper is to examine the effect of confinement and temperature-induced changes on vibrational states of CeO_{2-y} nanopowders using Raman spectroscopy. Here we have measured the Raman spectra (Stokes and anti-Stokes) of CeO_{2-y} nanocrystals in the temperature range from room temperature up to 1100 °C. We have found that in nano-CeO_{2-y} the temperature-induced Raman mode frequency shift consists of at least two contributions: the anharmonicity effect, on the one hand, and a phonon frequency change due to the change of nanoparticle size by temperature increase (confinement effect), on the other hand. The anti-Stokes/Stokes intensity ratio is smaller in nano-CeO_{2-y} powders in comparison with the polycrystalline sample. It is supposed that this difference comes from the change of the electronic structure of CeO_2 due to the change of the particle size induced by the temperature increase.

2. Experimental details

The self-propagating room temperature synthesis method was used to produce CeO_{2-y} nanocrystals of high quality with a narrow size particle distribution in the nanometric range. The details of the sample preparation procedure can be found in our recent publications [5–7]. Micro-Raman spectra were taken in backscattering configuration and analyzed using a Jobin Yvon T64000 spectrometer, equipped with a nitrogen cooled charge-coupled-device detector. As an excitation source we used the 514.5 nm and 488 nm lines of an Ar-ion laser. The high temperature measurements were performed using the Linkam TS 1500 microscope heating stage. Overheating of the sample was avoided by lowering the level of laser power on the sample till no changes of the Raman spectra were observed. The crystal structure of the CeO_{2-y} sample was identified using the powder x-ray diffraction (XRD) method on a Siemens D-5000 XRD diffractometer with Cu Kα radiation at room temperature. The average grain size was determined using the Scherrer formula $L = 0.941\lambda/B\cos\Theta$, where λ is the wavelength, B is the FWHM of the diffraction peak corrected using the corresponding peak of a micron-sized sample and Θ is the diffraction angle. The average size of CeO_{2-y} nanocrystals obtained from XRD measurements is $L = 6$ nm.

3. Results and discussion

Raman spectra (Stokes and anti-Stokes) of CeO_{2-y} nanocrystals, measured at different temperatures, are shown in figure 1. By heating, the Raman mode frequency continuously decreases and its line shape becomes less asymmetric, becoming totally symmetric at about 900 °C (see the right panel of figure 1).

The particle size effect provokes systematic changes in the Raman spectra of CeO_{2-y} when crystallite size decreases down to 6 nm [4, 6, 8]. The changes of the Raman mode position and shape in nanomaterials are usually studied using the phonon confinement model (PCM) [4, 9]. The evolution of the F_{2g} Raman mode (the mode frequency shift and broadening) strongly depends on the confinement and inhomogeneous strain effects due to the particle size distribution [4, 6]. With decreasing size, the Raman line shifts to lower energy becoming more asymmetric because of the contribution of interior phonons from the entire Brillouin zone ($q \neq 0$). According to this model, due to the relaxation of the $q \simeq 0$ selection rule in

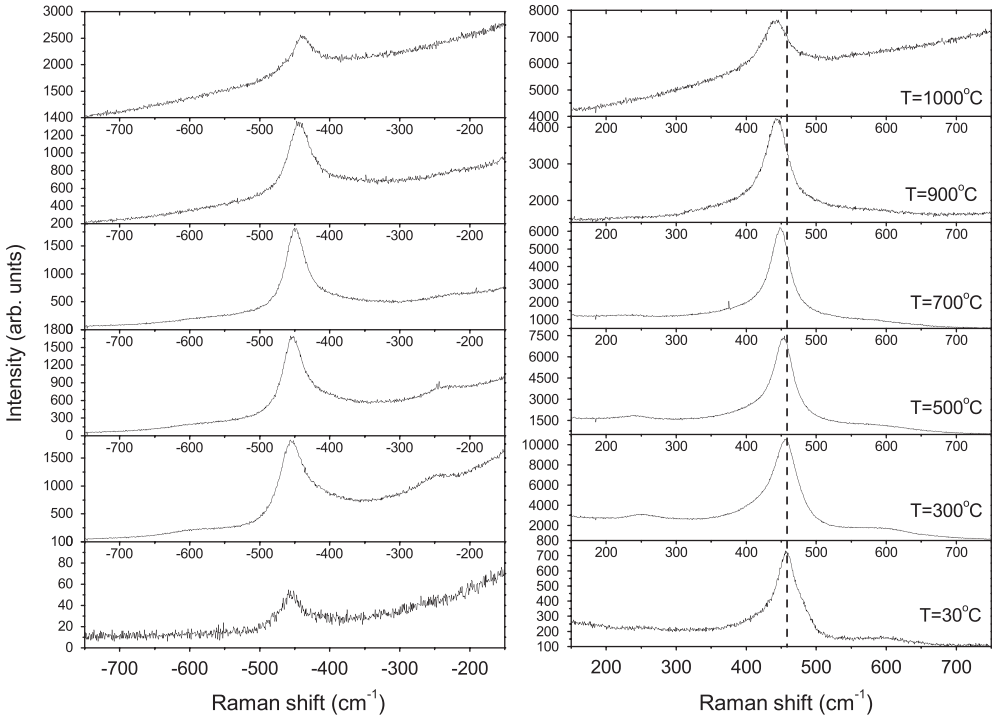

Figure 1. Stokes (right panel) and anti-Stokes (left panel) Raman spectra of CeO_{2-y} nanocrystals at different temperatures. Vertical broken line indicates a red shift of F_{2g} Raman active mode with increasing temperature.

finite size crystals, Raman intensity $I(\omega)$ is calculated over the whole Brillouin zone (assumed to be spherical) by the following relation [6]:

$$I(\omega) = \sum_{1}^{3} \int_{0}^{\infty} \rho(L)\,\mathrm{d}L \times \left(\int_{BZ} \exp\left(\frac{-q^2L^2}{8\beta}\right) \frac{\mathrm{d}^3q}{\{\omega - [\omega_i(q) + \Delta\omega_i(q, L)]\}^2 + (\Gamma_0/2)^2} \right) \mathrm{d}L, \qquad (1)$$

where the wavevector q is expressed in units of $2\pi/a$ (where a is the lattice constant of crystalline CeO_2), L is the particle diameter and Γ_0 is the intrinsic linewidth of the Raman mode in the bulk crystal. The factor β in equation (1) is an adjustable parameter that reflects the strength of the phonon confinement in the nanomaterials. In our calculations we used the value $\beta = 4\pi^2$. The best fit was obtained for $L = 7.8$ nm, which is in a rather good agreement with XRD results.

In the recent work of Mazali *et al* [10] regarding the Raman spectra of CeO_2 nanocrystals dispersed in porous Vycor glass, the authors used the same model as we did to estimate the particle size. Although they used a somewhat simplified dispersion relation model compared with ours [6], the obtained results are similar, demonstrating that the Raman method is a reliable characterization tool for estimating average nanocrystal size.

The Raman peak position is affected by a change of lattice parameter which, on the other hand, depends on particle dimension. The dispersion in particle size produces dispersion in lattice constant. This leads to an inhomogeneous strain and broadening of the Raman peak.

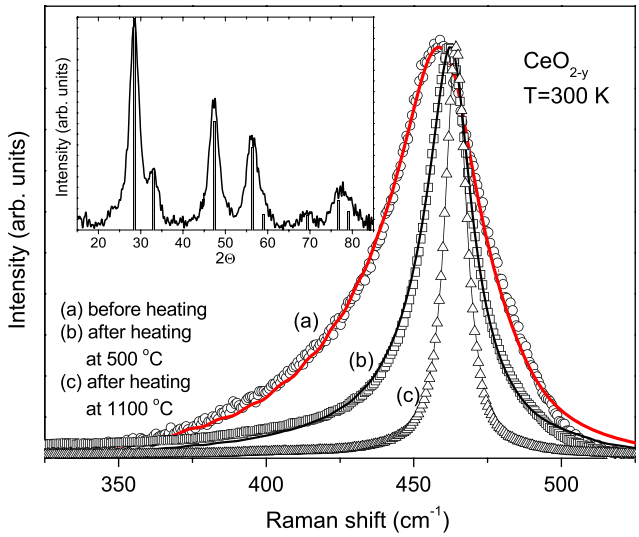

Figure 2. Room temperature Raman spectra of CeO_{2-y} nanocrystals before (open circles) and after different heat-treatment (open squares and triangles). Full lines ((a), (b)) are theoretical spectra obtained using equation (1) and a Lorentzian line profile fitting (c). Inset: room temperature x-ray diffraction patterns of CeO_{2-y} nanocrystals together with calculated XRD spectrum obtained for $a = 5.4122$ Å.

The effect of inhomogeneous strain is introduced into the model through the term $\Delta\omega_i(q, L)$ in equation (1), using the particle size distribution function to account for the shift and mode broadening. The sum is taken over three allowed Raman modes since the F_{2g} mode is triple degenerate. A large distribution of nanocrystalline sizes leads to a very large broadening and an asymmetry of the peak, as shown in detail in figure 2(a) (empty circles). In this case a good fit of the experimental line shape cannot be obtained in the framework of the phonon confinement model without including the particle size distribution function $\rho(L)$ in equation (1). We have already discussed in detail the use of this model concerning CeO_{2-y} nanocrystals in [6].

Although the CeO_{2-y} sample is not completely stoichiometric [5, 6] there is no indication that the oxygen deficiency greatly influences the position and linewidth of the F_{2g} Raman mode. According to McBride *et al* [11], with increasing disorder due to the presence of oxygen vacancies, the Raman mode will shift up in frequency (to higher energies) and this is not our case.

The x-ray diffraction patterns of CeO_{2-y} nanocrystals, the inset of figure 2, show a perfect crystallinity. It proves that our sample consists of nanosized CeO_2 single crystals, with no amorphous, defect or impurity phases. Such XRD spectra support the work of Hernandez *et al* where they deduced that the samples with average particle size between 3 and 10 nm have fluorite structure similar to the bulk while ceria nanoparticles below 3 nm are strongly disordered materials where the crystalline and amorphous domains exist [8].

In bulk materials, both the frequency and linewidth of optical phonons are found to vary with temperature. This temperature dependence can be attributed to anharmonic terms in the vibrational potential energy. Because of anharmonicity of the lattice forces, an optical mode can interchange energy with other lattice modes and in this way maintain thermal equilibrium. The principal anharmonic interactions are due to the cubic and quartic anharmonic terms, resulting in the splitting of the optical phonon into two or three acoustic phonons, respectively. According to Balkanski *et al* [12] the influence of these anharmonic effects on the Raman

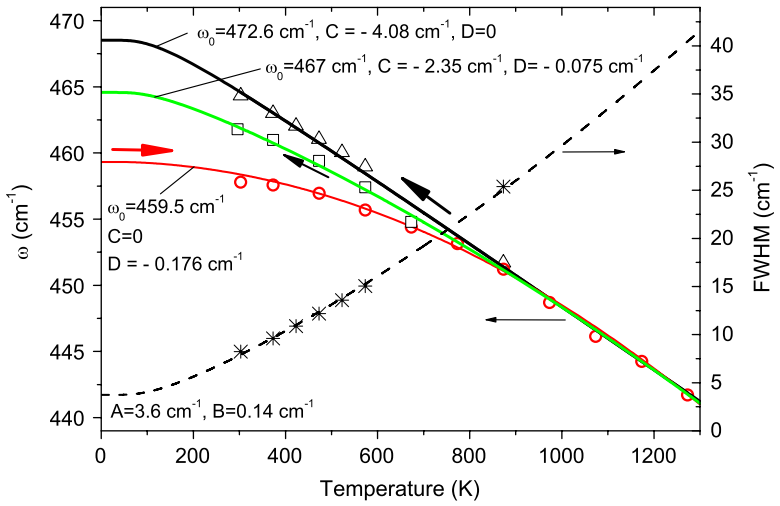

Figure 3. Frequency (circles, squares, triangles) and broadening (asterisks) of the F_{2g} Raman mode in CeO_{2-y} versus temperature. The solid (dashed) lines are calculated data using equations (2) and (3) with the fitting parameters indicated in the figure.

spectra in the materials under consideration is taken into account via three-and four-phonon decay processes:

$$\omega(q,T) = \omega_0 + C\left[1 + \frac{2}{e^{\hbar\omega_0/2k_BT} - 1}\right] + D\left[1 + \frac{3}{e^{\hbar\omega_0/3k_BT} - 1} + \frac{3}{(e^{\hbar\omega_0/3k_BT} - 1)^2}\right]. \quad (2)$$

The phonon linewidth is given by

$$\Gamma(T) = A\left[1 + \frac{2}{e^{\hbar\omega_0/2k_BT} - 1}\right] + B\left[1 + \frac{3}{e^{\hbar\omega_0/3k_BT} - 1} + \frac{3}{(e^{\hbar\omega_0/3k_BT} - 1)^2}\right], \quad (3)$$

where A, B, C, and D are anharmonic constants.

Since no theory of anharmonic effects has been developed yet for nanocrystals, we assume that the changes induced by temperature in the phonon vibrational states of the nanocrystals can be well described with the corresponding equations for bulk phonons (equations (2) and (3)).

Figure 3 shows the first-order Raman mode frequency of CeO_{2-y} nanocrystals at different temperatures. By heating, the Raman frequency continuously decreases (open circles in figure 3). In addition, as the temperature increases the line shape becomes less asymmetric, and at about 900 °C it is totally symmetric, as can be observed from figure 1. By cooling, the frequency of the F_{2g} mode increases (open triangles in figure 3), reaching the value of 464.3 cm^{-1} at room temperature. The linewidth (FWHM) decreases with temperature decrease down to 9 cm^{-1} at room temperature. These values are very close to the corresponding values of CeO_2 single crystals [13, 14], which leads us to conclude that our sample suffers a transformation from nano- to polycrystalline (see figure 2(c)) by the above-mentioned heating treatment. This means that all effects that arise from the nanometric size of the crystals, such as nonstoichiometry, inhomogeneous strain, confinement, structure defects, etc, are removed by heat treatment.

Equations (2) and (3) have been used to fit the experimental data by suitably choosing the constants ω_0, A, B, C, and D, and the agreement between the theoretical curve and experimental points is found to be quite good. It is natural to expect that in bulk materials the contribution of four-phonon processes should be small compared to that of the three-phonon processes [12], i.e. the ratios of B/A and D/C should be small (a few per cent). In

addition, in the high temperature limit, the factors multiplying C and D in equation (2) vary as T and T^2, respectively. Having this in mind, the results of the fitting procedure applied to the experimental frequency versus temperature dependence of nano-CeO_{2-y} are unexpected. Namely, as can be seen from figure 3, the Raman mode frequency of the nanocrystals (open circles) varies as T^2 ($C = 0$, $D = -0.176$ cm^{-1}), in the temperature range from 300–1300 K (high temperature limit). Consequently, we can conclude that, at least in CeO_{2-y} nanocrystals, the anharmonicity is dominated by four-phonon processes. The same fitting analysis applied to the polycrystalline CeO_2 sample (open triangles in figure 3) showed that a linear dependence with T ($C = -4.08$ cm^{-1}, $D = 0$, three-phonon processes) is more suitable for fitting the experimental data. The fact that the value of D for nanocrystals is much larger than that found in polycrystalline CeO_2 implies that the different phonon decay channels (four-phonon anharmonic effects) are more important in CeO_{2-y} nanocrystals than in the corresponding bulk. This conclusion could be valid only if the temperature dependence of other effects such as change of grain size (phonon confinement, inhomogeneous strain), or nonstoichiometry were not so important.

According to [15], no significant grain size increase was registered in nano-CeO_{2-y} with temperature increase up to 600 °C. Despite this, we believe that the frequency shift of the Raman mode in our nanocrystalline CeO_{2-y} sample with increasing temperature is also influenced by an increase in grain size. In order to verify this influence we heated the nano-CeO_{2-y} at 500 °C and measured the Raman spectra by cooling it down to room temperature. The corresponding peak frequencies are shown by open squares in figure 3, and the room temperature Raman spectrum, after the mentioned heat treatment, is shown in figure 2 (open squares). It is clear that Raman spectra before and after this heat treatment differ significantly. We fitted both of them with the phonon confinement model described by equation (1) and found that a starting grain size of about $L = 7.8$ nm is almost doubled ($L = 13$ nm) after annealing to 500 °C. Annealing at temperatures higher than 600 °C leads to a grain size increase up to $L = 22$ nm [5, 15], when the nanocrystalline sample transforms into the polycrystalline one. Room temperature Raman spectra of CeO_2 after annealing up to 1100 °C is displayed as open triangles in figure 2. This spectrum is totally symmetric with an absence of any of 'nano' effects, i.e. the line frequency and linewidth correspond to the values expected for bulk CeO_2. The ratio of the best fit anharmonicity parameters D/C reduces from 'pure' nano to 'pure' polycrystalline phase (see figure 3).

The above discussion should be considered with great care, since it is necessary to take into account that a temperature increase induces two opposite effects on the phonon frequency: a blue shift due to the grain size increase and a red shift due to anharmonicity. To determine which of these mechanisms dominates at different temperature ranges it would be necessary to compare Raman scattering with x-ray diffraction measurements performed on the same sample and at the same temperature. Namely, from the x-ray diffraction data it is possible to estimate the crystallite size (Scherrer equation) separating the effects of size and strain in nano-CeO_{2-y} samples using Williams–Hall plots [16]. Alternatively, a study implying only Raman scattering could be performed by repeating the heating/cooling cycles at various temperatures, and checking the increase of grain size by the use of the phonon confinement model to analyze the Raman shift at room temperature. In this work, this procedure is applied only at a temperature of 500 °C.

We checked the validity of the thermal effects on the phonon modes of the nanocrystals with an analysis of the relative intensities of Stokes and anti-Stokes scattering measured using 514.5 nm and 488 nm lines of an Ar-ion laser. In figure 4 we show the anti-Stokes/Stokes intensity ratio versus temperature for CeO_{2-y} nanocrystals as they are heated (open symbols) and cooled-down (full symbols). This ratio can be written as [12]

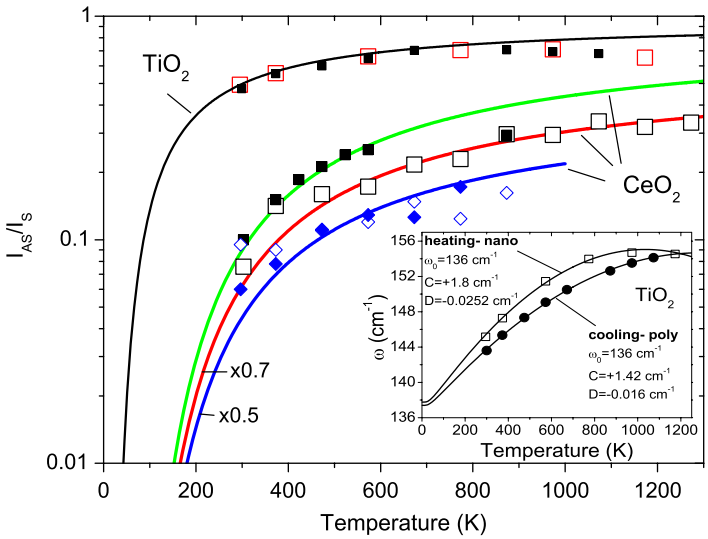

Figure 4. Temperature dependence of the anti-Stokes/Stokes intensity ratio for CeO_{2-y} and TiO_2 nanocrystalline samples, considering the corrections as discussed in the text. Open (solid) symbols represent data obtained by heating (cooling) of the samples. Squares (diamonds) represent green (blue) Ar-ion laser line measurements. The theoretical curves are represented by solid lines. Inset: frequency versus temperature dependence of E_g symmetry mode of a commercial TiO_2 nanocrystalline sample (grain size $\sim$ 5 nm). Solid lines are the best fit curves, equation (2), for anharmonic parameters indicated in the inset.

$$\frac{I_{\mathrm{AS}}}{I_{\mathrm{S}}} = A\left(\frac{\omega_{\mathrm{AS}}}{\omega_{\mathrm{S}}}\right)^3 \mathrm{e}^{-\hbar\omega_0/k_{\mathrm{B}}T}, \tag{4}$$

and

$$A = \frac{\alpha_{\mathrm{I}} + \alpha_{\mathrm{S}}}{\alpha_{\mathrm{I}} + \alpha_{\mathrm{AS}}} \frac{S(\omega_{\mathrm{I}}, \omega_{\mathrm{AS}})}{S(\omega_{\mathrm{I}}, \omega_{\mathrm{S}})}, \tag{5}$$

where α_{I}, α_{AS}, α_{S}, are the absorption constants at the incident (ω_{I}), anti-Stokes (ω_{AS}) and Stokes (ω_{S}) frequencies, whereas $S(\omega_{\mathrm{I}}, \omega_{\mathrm{AS}})$ and $S(\omega_{\mathrm{I}}, \omega_{\mathrm{S}})$ are the Raman cross sections at the involved frequencies.

In equation (5), A takes into account the frequency dependence of the absorption coefficient and Raman cross sections at the corresponding frequencies. Full lines in figure 4 represent the calculated spectra using equation (4). As can be seen from figure 4, the calculated spectrum for a polycrystalline CeO_2 sample fits well with the experimental values taking $A = 1$. For nano-CeO_{2-y} experimental data can be fitted with a correction coefficient which is about 30% smaller than for poly-CeO_2 ($A = 0.7$). We believe that this difference most probably comes from different absorption coefficients α_{AS}, α_{S} of nano-CeO_{2-y}. Support for this conclusion is found in [17, 18], where absorption coefficient as well as index of refraction versus wavelength of CeO_2 films are presented. There is a significant change of both quantities close to the laser line frequency of 514.5 nm. This means that the anti-Stokes/Stokes intensity ratio is strongly modulated due to a resonance Raman effect in the nano-CeO_{2-y} sample. With the blue line excitation of 488 nm (2.54 eV) resonance effects are even stronger, because the energy of this line is closer to the energy gap value of nanoceria. Ellipsometric or absorption coefficient measurements of nano-CeO_{2-y} at high temperatures can help to resolve this problem. Unfortunately these techniques are not at our disposal for the time being.

We check the validity of equation (4) in the case of commercial nano-TiO_2 (grain size $\sim$ 5 nm). As can be seen from figure 4, the anti-Stokes/Stokes intensity ratio does not change in the nano-(heating) and poly-(cooling) phase of TiO_2 and is well fitted with $A = 1$. Similarly to the case for our CeO_{2-y} sample, we find that the anharmonicity constants C and D as well as the D/C ratio are larger in the nanocrystals than in the polycrystalline phase of TiO_2 (see the inset of figure 4), although the changes observed are smaller than in nanocrystalline CeO_{2-y}.

A better knowledge of the correction factors is therefore necessary in order to use the anti-Stokes/Stokes ratio as a tool for the determination of temperature in nano-CeO_{2-y} samples. In the case of TiO_2, such correction is not necessary. From our measurements we conclude, however, that equation (4) may be applicable for temperature measurements in nanosized materials with similar restrictions as for the bulk samples.

4. Conclusion

In conclusion, we have found that at least two contributions are involved in the temperature-induced Raman mode frequency shift of nano-CeO_{2-y}: the anharmonicity effect and the phonon frequency change due to the change of nanoparticle size with temperature (confinement effect). The anti-Stokes/Stokes intensity ratio is smaller in CeO_{2-y} nanocrystals in comparison with the polycrystalline sample. This difference probably comes from the change of the electronic structure of CeO_2 due to the particle size change induced by the temperature increase, which changes the value of the absorption coefficients at the energies involved in the experiment.

Acknowledgments

This work was supported by the Serbian Ministry of Science under project no. 141047 and the OPSA-026283 Project within EC FP6 Programme. We would like to express our thanks to Dr B Matović and Dr S Bošković who provided us with some of the samples. Support from the Spanish Ministry of Education (MAT2006-01825-FEDER) is also acknowledged.

References

[1] Guadec G and Colomban P (eds) 2007 Raman study of nanomaterials *J. Raman Spectrosc.* **38** 597
[2] Mishra P and Jain K P 2000 *Phys. Rev.* B **22** 14790
[3] Konstantinović M J, Bersier S, Wang X, Hayne M, Lievens P, Silverans R E and Moshchalkov V V 2002 *Phys. Rev.* B **66** 161311(R)
[4] Spanier J E, Robinson R D, Zhang F, Chan S W and Herman I P 2001 *Phys. Rev.* B **64** 245407
Zhang F, Chan S W, Spanier J E, Apak E, Jin Q, Robinson R D and Herman I P 2002 *Appl. Phys. Lett* **80** 127
[5] Bošković S, Djurović D, Dohčević-Mitrović Z, Popović Z, Zinkevich M and Aldinger F 2005 *J. Power Sources* **145** 237
[6] Dohčević-Mitrović Z D, Šćepanović M, Grujić-Brojčin M, Popović Z V, Bošković S, Matović B, Zinkevich M and Aldinger F 2006 *Solid State Commun.* **137** 387
[7] Dohčević-Mitrović Z D, Grujić-Brojčin M, Šćepanović M, Popović Z V, Bošković S, Matović B, Zinkevich M and Aldinger F 2006 *J. Phys. Condes. Matter* **18** S2061
[8] Hernandez-Alonso M D, Hugria A B, Martinez-Arias A, Coronado J M, Conesa J C, Soria J and Fernandez-Garcia M 2004 *Phys. Chem. Chem. Phys.* **6** 3524
[9] Campbell I H and Fauchet P M 1986 *Solid State Commun.* **58** 739
[10] Mazali I O, Viana B C, Alves O L, Mendes Filho J and Souza Filho A G 2007 *J. Phys. Chem. Solids* **68** 622
[11] McBride J R, Hass K C, Poindexter B D and Weber W H 1994 *J. Appl. Phys.* **76** 2435
[12] Balkanski M, Wallis R F and Haro E 1983 *Phys. Rev.* B **28** 1928
[13] Sato T and Tateyama S 1982 *Phys. Rev.* B **26** 2257

[14] Weber W H, Hass K C and McBride J R 1993 *Phys. Rev.* B **48** 178
[15] Wang X, Hanson J C, Liu G, Rodriguez J A, Iglesias-Juez A and Fernandez-Garcia M 2004 *J. Chem. Phys.* **121** 5434
[16] Zhou X-D and Huebner W 2001 *Appl. Phys. Lett.* **79** 3512
[17] Kanakaraju S, Mohan S and Sood A K 1997 *Thin Solid Films* **305** 191
[18] Suzuki T, Kosacki I, Petrovsky V and Anderson U 2002 *J. Appl. Phys.* **91** 2308